

Nonequilibrium Spin Dynamics in a Trapped Fermi Gas with Effective Spin-Orbit Interactions

Tudor D. Stanescu, Chuanwei Zhang, and Victor Galitski

Condensed Matter Theory Center, Department of Physics, University of Maryland, College Park, Maryland 20742-4111, USA
(Received 28 March 2007; revised manuscript received 21 May 2007; published 14 September 2007)

We consider a trapped atomic system in the presence of spatially varying laser fields. The laser-atom interaction generates a pseudospin degree of freedom (referred to simply as *spin*) and leads to an effective spin-orbit coupling for the fermions in the trap. Reflections of the fermions from the trap boundaries provide a physical mechanism for effective momentum relaxation and nontrivial spin dynamics due to the emergent spin-orbit coupling. We explicitly consider evolution of an initially spin-polarized Fermi gas in a two-dimensional harmonic trap and derive nonequilibrium behavior of the spin polarization. It shows periodic echoes with a frequency equal to the harmonic trapping frequency. Perturbations, such as an asymmetry of the trap, lead to the suppression of the spin echo amplitudes. We discuss a possible experimental setup to observe spin dynamics and provide numerical estimates of relevant parameters.

DOI: [10.1103/PhysRevLett.99.110403](https://doi.org/10.1103/PhysRevLett.99.110403)

PACS numbers: 05.30.Fk, 03.75.Ss, 71.70.Ej, 72.25.Rb

Ultracold atomic gases have proven to be an ideal test ground for the experimental study of a variety of condensed matter phenomena [1]. A particularly interesting possibility is to realize spin-orbit (SO) interaction in cold atomic systems. In atomic gases, (pseudo)spin represents a combination of different hyperfine levels of atoms. It was proposed recently that motion of atoms in position-dependent laser configurations may give rise to an effective non-Abelian gauge potential [2–8]. As argued in this Letter, a similar setup may lead to an effective SO interaction. In particular, with proper laser configurations, one can engineer Rashba or linear Dresselhaus SO coupling terms as well as other types of couplings not accessible in solid state systems. The resulting spin dynamics in the adiabatic regime are remarkably simple, providing a robust experimental signature of the underlying effective SO coupling. Throughout this Letter, we refer to the pseudo-spin degree of freedom realized in cold-atom systems as simply *spin*.

One of the main aspects of spin dynamics in bulk condensed matter systems is the Dyakonov-Perel spin relaxation [9]. This mechanism involves random elastic scattering of electrons off of impurities. These scatterings lead to spin relaxation, which is a result of spin precession around a randomly oriented momentum-dependent axis. Another example is an electron in a quantum dot in the presence of SO coupling. In this case, the existence of discrete energy levels results in oscillatory time evolution of the spin polarization. The polarization decay and relaxation to an equilibrium state occur only in the presence of inelastic processes, such as electron-phonon interactions [10,11] or nuclear hyperfine effects [12,13]. In the absence of such processes, the relaxation due to scatterings off of the quantum dot boundary is qualitatively different from the bulk spin relaxation, as shown by the semiclassical analysis, e.g., of Chang *et al.* [14].

Atomic systems in the presence of spatially varying laser fields offer the new remarkable possibility of observing strongly nonequilibrium quantum spin dynamics in a

many-particle system without complications due to disorder that are always present in condensed matter systems. In addition, by changing the geometry of the trapping potential one can access various dynamic regimes characterized by either regular or chaotic behavior of the spin polarization [15,16]. In this Letter we concentrate on quantum spin dynamics of a Fermi gas confined in a two-dimensional harmonic trap and in the presence of a simple SO interaction term. We find that the spin polarization may show two qualitatively different behaviors dependent on the strength of the SO coupling and on the number of particles. In the strong coupling regime, the initially fully polarized Fermi gas becomes completely unpolarized within a short time and remains unpolarized most of the time. In the weak coupling regime, the spin polarization never vanishes but oscillates with the period $T = 2\pi/\omega$, determined by the harmonic trapping frequency, ω , with the oscillation amplitudes dependent on the SO coupling strength and the number of atoms. In both cases, spin polarization exhibits periodic echoes with the echo frequency equal to the harmonic trapping frequency. The echo amplitude and the period of spin polarization oscillations are strongly modified in an asymmetric elliptic harmonic trap.

Consider an ultracold Fermi gas confined in a quasi-two-dimensional (xy -plane) harmonic trap. Along the z direction, the atomic dynamics is “frozen” by a high frequency optical trap [17] or a deep optical lattice [18]. The SO coupling may be generated using the tripod scheme shown in Fig. 1(a), which is similar to the setup described in Ref. [5]. The states $|1\rangle$, $|2\rangle$, and $|3\rangle$ represent three degenerate hyperfine ground states (e.g., different Zeeman components of the hyperfine states of ${}^6\text{Li}$ atoms). These states are coupled to an excited state $|0\rangle$ by spatially varying laser fields L_{j0} , with the corresponding Rabi frequencies Ω_1 , Ω_2 , and Ω_3 . The single-particle Hamiltonian is

$$\hat{\mathcal{H}} = \mathbf{p}^2/2m + \hat{V}_{\text{trap}} + \hat{\mathcal{H}}_{a-l}, \quad (1)$$

where \mathbf{p} is the momentum, $\hat{V}_{\text{trap}} = \sum_j V_j(\mathbf{r})|j\rangle\langle j|$ represents

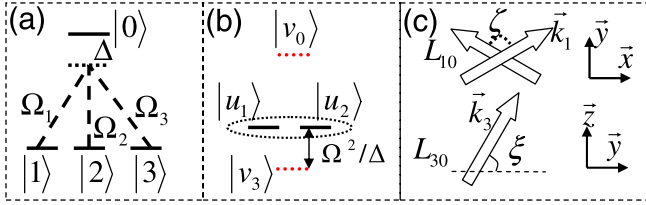


FIG. 1 (color online). Schematic representation of the experimental setup to create effective SO interaction. (a) Coupling between the lasers and the hyperfine states. (b) Energies of the degenerate dark states ($|u_i\rangle$) and of the bright states ($|v_i\rangle$). (c) Laser field configuration.

the position-dependent trapping potential, and $\hat{\mathcal{H}}_{a-l}$ is the laser-atom interaction Hamiltonian, given by $\hat{\mathcal{H}}_{a-l} = \Delta|0\rangle\langle 0| - [\Omega_1|0\rangle\langle 1| + \Omega_2|0\rangle\langle 2| + \Omega_3|0\rangle\langle 3| + \text{H.c.}]$, where Δ is the detuning to the excited state $|0\rangle$. The Rabi frequencies can be parametrized as $\Omega_1 = \Omega \sin\theta \cos\phi e^{iS_1}$, $\Omega_2 = \Omega \sin\theta \sin\phi e^{iS_2}$, and $\Omega_3 = \Omega \cos\theta e^{iS_3}$, with $\Omega = \sqrt{|\Omega_1|^2 + |\Omega_2|^2 + |\Omega_3|^2}$. We set $\hbar = 1$.

The diagonalization of $\hat{\mathcal{H}}_{a-l}$ yields four eigenstates: two degenerate dark states: $|u_1\rangle = \sin\phi e^{-iS_{13}}|1\rangle - \cos\phi e^{-iS_{23}}|2\rangle$, $|u_2\rangle = \cos\theta \cos\phi e^{-iS_{13}}|1\rangle + \cos\theta \sin\phi e^{-iS_{23}}|2\rangle - \sin\phi|3\rangle$ and two nondegenerate bright states: $|v_0\rangle \approx |0\rangle$ and $|v_3\rangle \approx \sin\theta \cos\phi e^{-iS_{13}}|1\rangle + \sin\theta \sin\phi e^{-iS_{23}}|2\rangle - \cos\theta|3\rangle$, with $S_{ij} = S_i - S_j$ [Fig. 1(b)]. Note that the energy of the dark states is not modified by the laser field. We assume $\omega \ll \Omega \ll \Delta$ and $\omega \ll \Omega^2/\Delta$, where ω is the characteristic frequency of the trapping potential, and we neglect contributions of order Ω/Δ and smaller. This condition implies that the states from the subspace spanned by $|u_1\rangle$ and $|u_2\rangle$ are well separated in energy from the states $|v_0\rangle$ and $|v_3\rangle$, so that the coupling between dark and bright states is negligible (adiabatic approximation). In the present work we concentrate on a particular configuration of laser fields [see Fig. 1(c)] characterized by $S_1 = S_2$, $S_{31} \equiv S = mv_s y$, $\phi = mv_\phi x$, and the constant angle $\theta \in [0, \pi]$. The laser field L_{10} is generated by two laser beams propagating in the xy plane and intersecting at an angle, ζ . These two lasers form a standing wave along the x direction and a plane wave along the y direction. The laser field L_{20} has the same configuration except that the standing wave along the x direction is shifted in phase by $\pi/2$. With such a setup, we have $\phi = 2k_1 x \sin(\zeta/2)$ [or $mv_\phi = 2k_1 \sin(\zeta/2)$] and $S_1 = S_2 = k_1 y \cos(\zeta/2)$, where $k_1 = k_2$ are the wave vectors for the laser beams. Finally, the laser field L_{30} is a plane wave propagating in the yz plane with an adjustable angle ξ with respect to the y axis, which leads to $S_3 = k_3 y \cos\xi$ [or $mv_s = k_3 \cos\xi - k_1 \cos(\zeta/2)$].

The effective low-energy Hamiltonian is obtained by projecting the Hamiltonian (1) onto the subspace of the degenerate dark states $|u_1\rangle \otimes |u_2\rangle$ [5]

$$\hat{\mathcal{H}}_u = \left[\frac{p^2}{2m} + w(r) \right] \hat{I}_2 + \delta_0 \hat{\sigma}_z + \hat{\mathcal{H}}_{\text{SO}}, \quad (2)$$

where \hat{I}_2 represents the 2×2 unit matrix and $\hat{\sigma}_j$ with $j \in \{x, y, z\}$ are the Pauli matrices. Here $V_1 = V_2 = w(r)$ and $V_3 = w(r) + \delta$, where $w(r) = m\omega^2 r^2/2$ (unless otherwise noted) is a symmetric harmonic potential and δ is a constant shift for the hyperfine state $|3\rangle$ that yields an effective Zeeman splitting $\delta_0 = \sin^2\theta[\delta - (v_s^2 + v_\phi^2)/2]/2$ of the dark states and can be varied through additional state-dependent laser fields [19]. The last term in (2) is the SO coupling

$$\hat{\mathcal{H}}_{\text{SO}} = -v_0 p_x \hat{\sigma}_y - v_1 p_y \hat{\sigma}_z, \quad (3)$$

with $v_0 = v_\phi \cos\theta$ and $v_1 = v_s \sin^2\theta/2$, where the pseudospin represents the internal degree of freedom associated with the degenerate dark states $|u_1\rangle$ and $|u_2\rangle$. We will call an atom in a $|u_1\rangle$ ($|u_2\rangle$) state as a spin-up (-down) particle. The term $\hat{\mathcal{H}}_{\text{SO}}$ of the effective Hamiltonian couples this (pseudo)spin degree of freedom to the motion of the atom inside the trap. The ‘‘direction’’ of the spin does not have any real space significance and is solely determined by the choice of the basis in the dark state subspace.

Atomic SO coupled systems open new possibilities to study strongly nonequilibrium spin dynamics in contrast to boundary linear response effects usually considered in solid state systems with SO coupling [20]. Below, we study such a problem for the simplest Ising-like spin orbit coupling, which already leads to a nontrivial dynamics. This choice corresponds to a constant phase $S = \text{const}$; i.e., the plane-wave components of the three laser fields L_{j0} along y direction share the same wave vector. We define the spin polarization $\mathcal{P}(t)$ as the difference between the occupation numbers of the dark states $|u_1\rangle$ and $|u_2\rangle$. We assume that at $t = 0$, the system is fully polarized $\mathcal{P}(0) = 1$; i.e., all the particles are in the dark state $|u_1\rangle$. The corresponding single-particle quantum mechanics problem, which can be easily solved exactly. If $\phi_\alpha(\mathbf{r})$ is an eigenstate of the operator $H_0 = p^2/2m + w(\mathbf{r})$ with an eigenvalue ϵ_α , then the eigenfunction of the SO coupled Hamiltonian $\hat{\mathcal{H}}_u = H_0 \hat{I}_2 - v_0 p_x \hat{\sigma}_y$ is

$$\bar{\psi}_{\alpha\lambda}(\mathbf{r}) = \phi_\alpha(\mathbf{r}) e^{i\lambda m v_0 x} \frac{1}{\sqrt{2}} \begin{pmatrix} 1 \\ i\lambda \end{pmatrix}, \quad (4)$$

with $\lambda = \pm 1$. For a harmonic trap, $w(r) = m\omega^2 r^2/2$, $\phi_\alpha(\mathbf{r}) = \varphi_{n_x}(x) \varphi_{n_y}(y)$ can be written as a product of the harmonic oscillator eigenfunctions φ_n and the energy spectrum becomes $\epsilon_{n_x n_y} = \omega(n_x + n_y + 1)$. The eigenfunctions (4) are degenerate with respect to λ and have the eigenvalues $E_\alpha = \epsilon_\alpha - mv_0^2/2$.

Next, we define the spin polarization $\mathcal{P}(t) = \frac{1}{N} \times \langle \Phi(t) | \hat{P}_z | \Phi(t) \rangle$ as the average over the quantum many-body state $\Phi(t)$ obtained from the initial state Φ_0 by applying the time evolution operator $\hat{U}(t) = \exp(-i\hat{\mathcal{H}}t)$. The operator \hat{P}_z can be expressed in terms of field operators $\hat{\Psi}(\mathbf{r})$ as $\hat{P}_z = \int d^2r \hat{\Psi}^\dagger(\mathbf{r}) \hat{\sigma}_z \hat{\Psi}(\mathbf{r})$. In the Heisenberg representation, the polarization becomes $\hat{P}_z(t) = \hat{U}^{-1}(t) \hat{P}_z \hat{U}(t)$. We can ob-

tain the explicit time dependence by expressing the field operators in terms of creation and annihilation operators associated with the single particle eigenstates (3), $\hat{\Psi}(\mathbf{r}) = \sum_{\alpha,\lambda} \bar{\psi}_{\alpha\lambda}(\mathbf{r}) \hat{a}_{\alpha\lambda}$, and taking advantage of the simple time dependence of these operators, $\hat{a}_{\alpha\lambda}(t) = \hat{a}_{\alpha\lambda} e^{-iE_{\alpha}t}$. In order to evaluate the action of the polarization operator on $|\Phi_0\rangle$, it is convenient to introduce a set of operators $\hat{b}_{\alpha\sigma}$ associated with the fully polarized single-particle states $\bar{\psi}_{\alpha\sigma}^{(0)}(\mathbf{r}) = \phi_{\alpha}(\mathbf{r}) \bar{\chi}_{\sigma}$, with $\bar{\chi}_{\uparrow}^{\dagger} = (1, 0)$ and $\bar{\chi}_{\downarrow}^{\dagger} = (0, 1)$ and satisfying the relation $\hat{b}_{\alpha\sigma} = \sum_{\beta\lambda} \langle \bar{\psi}_{\alpha\sigma}^{(0)} | \bar{\psi}_{\beta\lambda} \rangle \hat{a}_{\beta\lambda}$. In terms of the b -type operators, the initial state can be written as $|\Phi_0\rangle = \prod_{\alpha} \hat{b}_{\alpha\uparrow}^{\dagger} |\emptyset\rangle$, where $|\emptyset\rangle$ represents the vacuum and the prime signifies that the product is constrained by the condition $E_{\alpha} \leq E_F$, where $E_F = \omega(N_F + 1)$ is the ‘‘Fermi’’ energy. After recasting $\hat{P}_z(t)$ in terms of b -type operators, the polarization becomes

$$\mathcal{P}(t) = \frac{1}{2N} \sum_{\sigma,\alpha,\beta} \sum_{\gamma}^{(E_{\gamma} \leq E_F)} \langle \phi_{\gamma} | e^{i\sigma\xi} | \phi_{\alpha} \rangle \langle \phi_{\alpha} | e^{-2i\sigma\xi} | \phi_{\beta} \rangle \times \langle \phi_{\beta} | e^{i\sigma\xi} | \phi_{\gamma} \rangle e^{i(\epsilon_{\alpha} - \epsilon_{\beta})t}, \quad (5)$$

where $\xi = mv_0x$ and $\sigma = \pm 1$. Equation (5) expresses the polarization of a noninteracting many-body system with SO interaction in terms of matrix elements of the single-particle states ϕ_{α} describing the motion of an atom in the confining potential. The effects of the SO coupling are contained in the parameter ξ and the finite number of particles enters through the constraint on the γ sum. Equation (5) contains matrix elements $\langle \varphi_n | e^{-2i\sigma\xi} | \varphi_m \rangle$ of the harmonic eigenfunctions $\varphi_n(x)$ with energies $\epsilon_n = \omega(n + 1/2)$. The summations over the quantum numbers are performed numerically. The time dependence of the pseudospin polarization for N particles that are initially in the dark state $|u_1\rangle$ and occupy the first N_F energy levels is shown in Fig. 2. We parametrize the strength of the SO coupling by $\alpha = (mv_0^2/2\hbar\omega)^{1/2}$. Notice that all the curves in Fig. 2 display a periodic structure.

Spin relaxation depends strongly on both the strength of the SO interaction (i.e., on α) and the number of particles (i.e., on N_F). In the weak coupling limit, $\alpha^2 N_F \ll 1$, the polarization deviates slightly from unity and we have

$$\mathcal{P}(t) \approx 1 - 4\alpha^2 \left(\frac{2N_F}{3} + 1 \right) [1 - \cos(\omega t)]. \quad (6)$$

At strong coupling, $\alpha^2 N_F \gg 1$, the polarization is characterized by fast spin relaxation to zero and periodic spin echoes that restore \mathcal{P} to its initial value. Performing a power expansion of the polarization at small times we get

$$\mathcal{P}(t) \approx 1 - \sum_n c_n (\alpha \sqrt{N_F} \omega t)^{2n}, \quad (7)$$

where c_n are numerical coefficients. From this we obtain the time scale of the fast relaxation, $\Delta t = 1/(\omega \alpha \sqrt{N_F})$, which is also the characteristic width of the echo peaks.

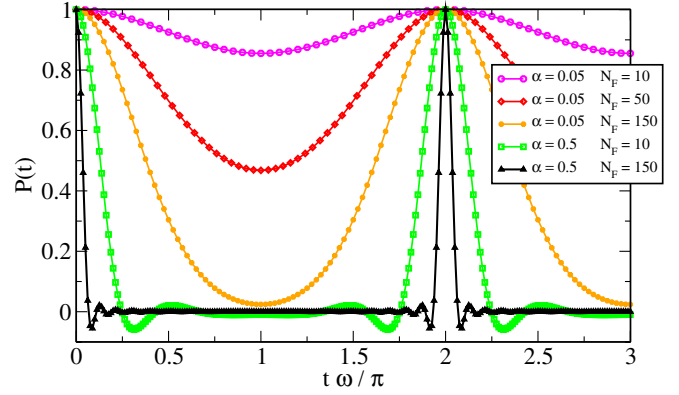


FIG. 2 (color online). Spin polarization as a function of time. Relaxation curves are plotted for $N = (N_F + 1)(N_F + 2)/2$ particles in a harmonic trap and in the presence of a (pseudo) SO interaction parametrized by $\alpha = (mv_0^2/2\omega)^{1/2}$. The $2\pi/\omega$ periodicity is due to the equal spacing between the harmonic oscillator levels. When $\alpha N_F^{1/2}$ is large (black curve with triangles), the polarization is characterized by fast relaxation followed by periodic echoes.

The relaxation to zero polarization in the strong coupling limit is a nontrivial dynamical effect. In Eq. (5), we can separate explicitly the time-independent contributions coming from the states with $\epsilon_{\alpha} = \epsilon_{\beta}$ and write the polarization as $\mathcal{P}(t) = P_{\text{const}} + \Delta P(t)$. For large but finite values of the parameter $\alpha \sqrt{N_F}$ the time-independent contribution P_{const} does not vanish. Instead, after the initial relaxation, the time-dependent term approaches a constant value, $\Delta P(t) \rightarrow -P_{\text{const}}$, leading to a vanishing polarization. The time-independent contribution P_{const} is shown in Fig. 3 for different sets of parameters (α, N_F). Notice that in the large coupling limit P_{const} depends on a single scaling parameter, $\alpha \sqrt{N_F}$. In fact, as it is suggested by

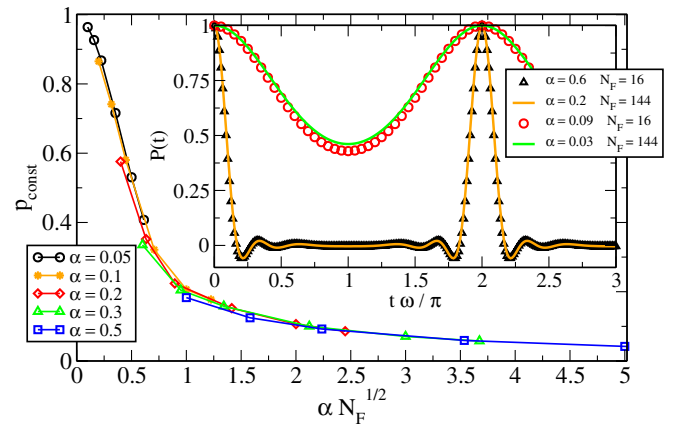


FIG. 3 (color online). The time-independent contribution to the polarization as a function of the effective coupling parameter $\alpha N_F^{1/2}$. For each α , P_{const} was determined for several values of N_F . In the strong coupling limit P_{const} scales with $\alpha N_F^{1/2}$. Inset: relaxation curves for sets of parameters corresponding to the same effective coupling: $\alpha N_F^{1/2} = 2.4$ (black triangles and orange line) and $\alpha N_F^{1/2} = 0.36$ (red circles and dashed green line).

Eq. (7), the polarization itself scales with $\alpha\sqrt{N_F}$ in the strong coupling limit (see the inset of Fig. 3).

The periodic time dependence of the polarization is a consequence of the equidistant energy spectrum. What would be the result of altering this structure? We consider an elliptical trap described by the potential $w(\mathbf{r}) = m[\omega_1^2(x\cos\chi - y\sin\chi)^2 + \omega_2^2(x\sin\chi + y\cos\chi)^2]/2$, where the angle χ describes the orientation of the symmetry axes of the trap potential relative to the (x, y) directions defined by the laser field. If $\chi = 0$ ($\chi = \pi/2$), $\mathcal{P}(t)$ is the same as for an isotropic system with a trap frequency ω_1 (ω_2). If the orientation of the symmetry axes deviates from the (x, y) directions, $\mathcal{P}(t)$ is still periodic if ω_2/ω_1 is a rational number and nonperiodic otherwise. In the former case with $\omega_2/\omega_1 = p/q$, the period of oscillations is $T = p(2\pi/\omega_2) = q(2\pi/\omega_1)$ (see Fig. 4). Notice that in the weak coupling regime (upper panel in Fig. 4) for small deviations from the symmetry axes, spin relaxation is reminiscent of the periodic structure of the symmetric configuration. However, the residual echoes become weaker and eventually vanish in the strong coupling limit (lower panel in Fig. 4).

Finally, we briefly discuss how to observe spin relaxation and echoes in ultracold Fermi gases through time of flight measurements. Initially the atoms are prepared in the state $|1\rangle$. To transfer them to the spin up polarized state $|u_1\rangle$, one applies a Raman pulse between the states $|1\rangle$ and $|2\rangle$ with a spatially dependent Rabi frequency that matches the spatial variation of the $|u_1\rangle$ state. Then, the laser fields L_{i0} are turned on and the Fermi gas experiences the effective SO coupling. After a certain time t , one turns off the

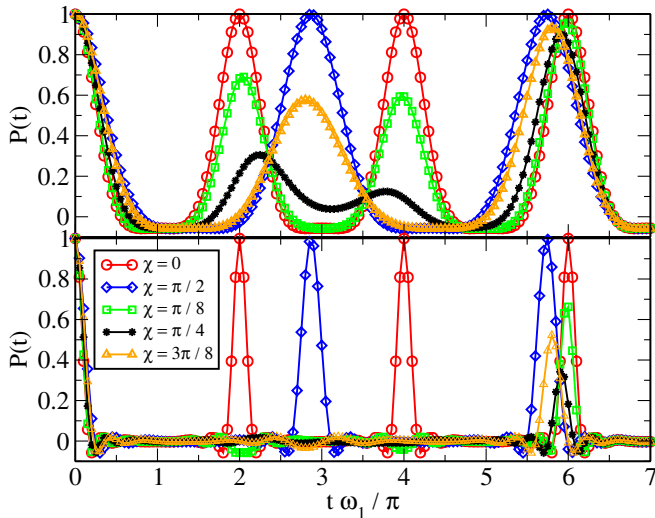


FIG. 4 (color online). Spin polarization as a function of time in an elliptic harmonic trap (with $\omega_2/\omega_1 = 23/33$). Relaxation curves are plotted for different laser orientations parametrized by the angle χ (see text). The upper and lower panels correspond to the SO couplings $\alpha = 0.2$ and $\alpha = 0.6$, respectively. For an arbitrary orientation of the lasers, $\mathcal{P}(t)$ has a period $23(2\pi/\omega_2) = 33(2\pi/\omega_1)$. The residual echoes become smaller and eventually vanish in the strong coupling limit.

laser fields L_{i0} and applies a reversal Raman pulse to transfer the atoms from $|u_1\rangle$ back to $|1\rangle$. Finally, a time of flight measurement gives the number of atoms in the $|1\rangle$ state (i.e., in $|u_1\rangle$ at time t) and thus determines the spin polarization $\mathcal{P}(t)$. A possible choice of parameters is $\omega = 2\pi \times 10$ Hz, $\Delta = 2\pi \times 10^2$ GHz, and $\Omega = 2\pi \times 10^7$ Hz, satisfying $\omega \ll \Omega \ll \Delta$ and $\omega \ll \Omega^2/\Delta$. The strength of the SO coupling $v_0 = v_\phi \cos\theta = \frac{2\hbar k_1}{m} \sin(\frac{\zeta}{2}) \times \cos\theta$ can be varied from 0 to $\frac{2\hbar k_1}{m} \cos\theta$ by adjusting the angle ζ between the laser beams. Consequently, $\alpha = (mv_0^2/2\hbar\omega)^{1/2} = 2(\omega_r/\omega)^{1/2} \sin(\frac{\zeta}{2}) \cos\theta$ (where ω_r is the photon recoil frequency for L_{10}) can vary in a range from 0 to 100 for ${}^6\text{Li}$ atoms. Therefore, both the strong and weak SO coupling limits are accessible in experiment.

C. Z. was supported by ARO-DTO, ARO-LPS, and LPS-NSA.

- [1] M. Lewenstein, A. Sanpera, V. Ahufinger, B. Damski, A. Sen De, and U. Sen, *Adv. Phys.* **56**, 243 (2007).
- [2] G. Juzeliunas and P. Ohberg, *Phys. Rev. Lett.* **93**, 033602 (2004).
- [3] G. Juzeliunas, P. Ohberg, J. Ruseckas, and A. Klein, *Phys. Rev. A* **71**, 053614 (2005).
- [4] D. Jaksch and P. Zoller, *New J. Phys.* **5**, 56 (2003).
- [5] J. Ruseckas, G. Juzeliunas, P. Ohberg, and M. Fleischhauer, *Phys. Rev. Lett.* **95**, 010404 (2005).
- [6] K. Osterloh, M. Baig, L. Santos, P. Zoller, and M. Lewenstein, *Phys. Rev. Lett.* **95**, 010403 (2005).
- [7] S. Zhu, H. Fu, C. Wu, S. Zhang, and L. Duan, *Phys. Rev. Lett.* **97**, 240401 (2006).
- [8] I. I. Satija, D. C. Dakin, and C. W. Clark, *Phys. Rev. Lett.* **97**, 216401 (2006).
- [9] M. I. Dyakonov and V. I. Perel, *Zh. Eksp. Teor. Fiz.* **60**, 1954 (1971) [*Sov. Phys. JETP* **33**, 1053 (1971)].
- [10] A. V. Khaetskii and Y. V. Nazarov, *Phys. Rev. B* **61**, 12 639 (2000).
- [11] L. Woods, T. Reinecke, and Y. Lyanda-Geller, *Phys. Rev. B* **66**, 161318 (2002).
- [12] I. Merkulov, A. Efros, and M. Rosen, *Phys. Rev. B* **65**, 205309 (2002).
- [13] Y. Semenov and K. Kim, *Phys. Rev. Lett.* **92**, 026601 (2004).
- [14] C. Chang, A. Mal'shukov, and K. Chao, *Phys. Rev. B* **70**, 245309 (2004).
- [15] V. Milner, J. Hanssen, W. Campbell, and M. Raizen, *Phys. Rev. Lett.* **86**, 1514 (2001).
- [16] N. Friedman, A. Kaplan, D. Carasso, and N. Davidson, *Phys. Rev. Lett.* **86**, 1518 (2001).
- [17] T. P. Meyrath, F. Schreck, J. L. Hanssen, C. Chuu, and M. Raizen, *Phys. Rev. A* **71**, 041604 (2005).
- [18] I. Spielman, W. Phillips, and J. Porto, *Phys. Rev. Lett.* **98**, 080404 (2007).
- [19] R. Grimm, M. Weidemuller, and Y. Ovchinnikov, *Adv. At. Mol. Opt. Phys.* **42**, 95 (2000).
- [20] E. G. Mishchenko, A. V. Shytov, and B. I. Halperin, *Phys. Rev. Lett.* **93**, 226602 (2004); V. M. Galitski, A. A. Burkov, and S. Das Sarma, *Phys. Rev. B* **74**, 115331 (2006).